Eur. Phys. J. B **2**, 225–232 (1998)

THE EUROPEAN PHYSICAL JOURNAL B

Slowing down in the three-dimensional three-state Potts glass with nearest neighbor exchange $\pm$ J: A Monte Carlo study

M. Reuhl, P. Nielaba[a], and K. Binder

Institut für Physik, Johannes Gutenberg-Universität Mainz, Staudingerweg 7, 55099 Mainz, Germany

Received: 8 October 1997 / Accepted: 27 November 1997

Abstract. ‚Static and dynamic properties of the Potts model on the simple cubic lattice with nearest neighbor $\pm\hat{J}$-interaction are obtained from Monte Carlo simulations in a temperature range where full thermal equilibrium still can be achieved ($T/\hat{J} \geq 0.6$). For a lattice size $L = 16$, in this range finite size effects are still negligible, but the data for the spin glass susceptibility agree with previous extrapolations based on finite size scaling of very small lattices. While the static properties are compatible with a zero temperature transition, they certainly do not prove it. Unlike the Ising spin glass, the decay of the time-dependent order parameter is compatible with a simple Kohlrausch function, $q(t) \propto \exp[-(t/\tau)^{y(T)}]$, while a power law prefactor cannot be distinguished. The Kohlrausch exponent $y(T)$ decreases from $y \approx 0.64$ at $T/\hat{J} = 1.1$ to $y \approx 0.37$ at $T/\hat{J} = 0.6$, however. The relaxation time τ is compatible with the exponential divergence postulated by McMillan for spin glasses at their lower critical dimension, $\ln\tau \propto T^{-\sigma}$ but the exponent σ that can be extracted ($\sigma \approx 2.5$) still differs significantly from the theoretical value, $\sigma = 3$. Thus the present results support the conclusion that the Potts spin glass in $d = 3$ dimensions differs qualitatively from the Ising spin glass.

PACS. 64.60.Cn Order-disorder transformations; statistical mechanics of model systems – 75.50.Lk Spin glasses and other random magnets – 02.70.Lq Monte-Carlo and statistical methods

1 Introduction

Spin glasses still are interesting model systems that elucidate how the interplay of quenched disorder and frustration lead to new types of ordering phenomena in condensed matter [1–4]. Nevertheless, many aspects of spin glasses are not yet well understood: while there is some consensus among researchers (though the evidence is not beyond doubt) that the Ising spin glass with short range forces has a non-zero freezing temperature T_f and hence its lower critical dimension $d_\mathrm{l} < 3$, the nature of the phase appearing for $T < T_\mathrm{f}$ still is heavily debated [4]. In contrast, it has been suggested [5–9] that the three-state Potts glass with short range forces is at its lower critical dimension, with $T_\mathrm{f} = 0$ in $d = d_\mathrm{l} = 3$. This claim is rather surprising – one could have expected that all spin glass models with a discrete number of spin states behave qualitatively similar (in mean field theory indeed the properties of the Ising spin glass and the Potts spin glass with $p = 3$ states are qualitatively similar, while for $p > 4$ a first order glass transition is predicted [5,6]). Main evidence for this conclusion that $d_\mathrm{l} = 3$ for the short range $p = 3$ Potts glass has been the lack of an intersection point for the cumulant of the spin glass order parameter when studied as function of temperature for different (small) lattice linear dimensions L [5–9]. In retrospect, however, this evidence seems rather weak, since no such intersection point is also found for the $p = 3$ infinite range Potts glass [10], where one knows exactly that T_f is nonzero [5,6,11]!

In view of these problems, a direct analysis of the properties of the Potts glass with short range interactions that does not rely on finite size scaling [12] seems rewarding: Choosing a lattice with linear dimension L exceeding by far the spin glass correlation length $\xi_\mathrm{SG}(T)$ for the temperatures T that are studied, one can ignore finite size effects and study $\xi_\mathrm{SG}(T)$, the spin glass susceptibility and the dynamic behavior of the model and try to extrapolate these quantities to lower temperatures. Such an analysis, complementary to finite size scaling, has proven to be very powerful and useful in the case of the $d = 3$ Ising spin glass [13,14]. While a related approach has been tried for the $d = 3$ Potts glass with nearest-neighbor random Gaussian interaction [15], the present paper is the first attempt of this type for the $d = 3 \pm J$ Potts glass. In this context, we note that (i) it is unclear whether at the lower critical dimension different distributions of the random exchange couplings yield equivalent results, and (ii) reference [15] has applied significantly less statistical effort than nowadays is possible (choosing $L = 12$ and 80 random bond configurations for runs that went at most up to 10^6 attempted Monte Carlo steps per spin [15], while the present

[a] *Present address*: Institut für Theoretische Physik, Universität des Saarlandes, Postfach 151150, 66041 Saarbrücken, Germany, e-mail: nielaba@cleopatra.physik.uni-mainz.de

effort is about two orders of magnitude larger, see below). In addition, the present work uses the technique of Bhatt and Young [16] to check whether the initial states included in the Monte Carlo average are well enough equilibrated, and thus unlike reference [15] does not suffer from possibly insufficient thermal equilibrium.

In Section 2 we briefly summarize the model, the simulation technique, and define the quantities that are recorded. Section 3 describes the results for static properties (including also linear and both second order and third order nonlinear "ferromagnetic" susceptibilities [17]). Section 4 then presents a discussion of the decay of the time-dependent Edwards-Anderson [18] order parameter $q(t)$ and associated relaxation time [19]. Particular attention is paid to a test of the pertinent predictions of McMillan [20] for the dynamics of spin glasses at the lower critical dimensionality. Finally, Section 5 summarizes our conclusions.

2 Model and simulation techniques

As is well known [21,22], in the Potts model an energy $\hat{J}_{ij}$ is won if two sites i, j are in the same state while no energy occurs if they are in different states, allowing $n_i = 1, 2, ..., p$ different states for each site i,

$$\mathcal{H} = -\sum_{\langle i,j \rangle} \hat{J}_{ij} \delta_{n_i,n_j} - \hat{h} \sum_i \delta_{n_i,1}. \tag{1}$$

Here we have specialized already to the case of a nearest neighbor interaction, so the symbol $\langle i,j \rangle$ means over all nearest neighbor pairs on the simple cubic lattice is summed once, and we have added a uniform field $\hat{h}$ that singles out one state (which we label as $n_i = 1$). In order to clearly bring out the symmetries of the model, it is convenient to choose the "simplex representation" [23], *i.e.* the p states n_i correspond to $(p-1)$-dimensional unit vectors pointing towards the λ'th corner of a p-simplex:

$$\mathbf{S}_i^{(\lambda)} \cdot \mathbf{S}_j^{(\lambda')} = \frac{p\delta_{\lambda\lambda'} - 1}{p-1}; \quad \lambda, \lambda' = 1, ..., p. \tag{2}$$

For $p = 3$ the space of the three vectors $\mathbf{S}_i^{(1)}$, $\mathbf{S}_i^{(2)}$, $\mathbf{S}_i^{(3)}$ representing the states $n_i = 1, 2, 3$ at site i is two-dimensional and their x, y coordinates are denoted as $\{S_i^u\} = \left(S_i^1, S_i^2\right)$. These vectors then read as follows

$$\begin{aligned} \mathbf{S}_i^{(1)} &= (0, 1), \\ \mathbf{S}_i^{(2)} &= \left(\frac{\sqrt{3}}{2}, \frac{-1}{2}\right), \\ \mathbf{S}_i^{(3)} &= \left(-\frac{\sqrt{3}}{2}, \frac{-1}{2}\right). \end{aligned} \tag{3}$$

In the simplex representation the Hamiltonian looks like that of a $(p-1)$ vector model,

$$\mathcal{H} = -\sum_{\langle i,j \rangle} J_{ij} \mathbf{S}_i \cdot \mathbf{S}_j - h \sum_i S_i^y, \tag{4}$$

but one must keep in mind that the $\mathbf{S}_i$ in equation (4) are the discrete vectors of equation (3) and thus $\mathcal{H}$ lacks spin inversion symmetry (except for $p = 2$, which is equivalent to the Ising case). Since for $p = 3$ we simply have $\delta_{n_i,n_j} = \frac{2}{3}\left(\mathbf{S}_i \cdot \mathbf{S}_j + \frac{1}{2}\right)$, $J_{ij} = \frac{2}{3}\hat{J}_{ij}$ and $h = \frac{2}{3}\hat{h}$. Note that J_{ij} is chosen as $+J$ and $-J$ with equal probability, while h is usually taken to be zero.

Next we define the quantities that will be discussed in this work. The correlation function that measures spin glass-type correlations is defined as usual [1,6]

$$g(r) = \left[\langle \mathbf{S}_i \cdot \mathbf{S}_j \rangle_T^2\right]_{\rm av}, \; r = |\mathbf{R}_i - \mathbf{R}_j|. \tag{5}$$

Here $\langle ... \rangle_T$ denotes the standard thermal average, implying an average with the Boltzmann weight $\exp(-\mathcal{H}/k_{\rm B}T)$, while $[...]_{\rm av}$ is the average over the quenched disorder, *i.e.* a simple sampling over a number $\mathcal{N}$ of realizations of the random bond configurations $\pm J$ in the lattice. We typically choose $\mathcal{N} = 128-200$. Obviously, the random bond averaging can be trivially done in parallel, and hence the use of parallel computers has turned out to be very advantageous for the present study (a CONVEX SPP1200 was used). At a single workstation (Hewlett Packard HP 9000/735) the total computing time would have exceeded 9 months of CPU time.

From $g(r)$ one can define a "second moment" correlation length $\xi_{\rm SG}(T)$ as follows,

$$\xi_{\rm SG}^2(T) = \frac{1}{6} \frac{\int {\rm d}^3 r \; r^2 g(r)}{\int {\rm d}^3 r \; g(r)}; \tag{6}$$

the denominator in equation (6) is nothing else but the spin glass susceptibility $\chi_{\rm SG}$, N being the total number of sites ($N = L^3$),

$$\chi_{\rm SG} = \frac{1}{N} \sum_{i,j} \left[\langle \mathbf{S}_i \cdot \mathbf{S}_j \rangle_T^2\right]_{\rm av}, \tag{7}$$

since $\int {\rm d}^3 r$ stands symbolically for a summation over all (vectorial) distances $\mathbf{R}_i - \mathbf{R}_j$ on the lattice.

In addition, we are also interested in ferromagnetic susceptibilities defined from the expansion of $m_y(h,T)$ in powers of $h/k_{\rm B}T$,

$$m_y(h,T) = \frac{1}{N} \sum_i \left[\langle S_i^y \rangle_{T,h}\right]_{\rm av} = \left[\langle m_y \rangle_{T,h}\right]_{\rm av}, \tag{8}$$

$$m_y(h,T) = \chi_1(h/k_{\rm B}T) + \chi_2(h/k_{\rm B}T)^2 + \chi_3(h/k_{\rm B}T)^3 + ... \tag{9}$$

Note that in conventional magnetic systems spin inversion symmetry implies $\chi_2 \equiv 0$, while in the Potts glass lack of spin inversion symmetry implies that χ_2 indeed is nonzero [17]. While Haas *et al.* [17] attempted to obtain χ_1, χ_2 and χ_3 from calculations for a set of values for nonzero h and a numerical fit of $m_y(h,T)$ *vs.* h curves to the expansion, equation (9), it turned out that this procedure is numerically rather unstable, depending on

the range of values for h that is fitted: if this range is too large, even higher order terms than written down in equation (4) contribute, while if this range is too small the nonlinear terms hardly have any effect. Therefore, in the present study we implemented the alternative approach in terms of the fluctuation relations for $h = 0$

$$\chi_1 = N\left[\langle m_y^2\rangle_T - \langle m_y\rangle_T^2\right]_{\rm av}, \tag{10}$$

$$\chi_2 = \frac{1}{2!}N^2\Big\{\left[\langle m_y^3\rangle_T - 3\langle m_y^2\rangle_T\langle m_y\rangle_T + 2\langle m_y\rangle_T^3\right]_{\rm av}\Big\}, \tag{11}$$

$$\chi_3 = \frac{1}{3!}N^3\{[\langle m_y^4\rangle_T - 4\langle m_y\rangle_T\langle m_y^3\rangle_T + 12\langle m_y^2\rangle_T\langle m_y\rangle_T^2 - 3\langle m_y^2\rangle_T^2 - 6\langle m_y\rangle_T^4]_{\rm av}\}. \tag{12}$$

Remember that in magnetic spin glasses (where $\chi_2 \equiv 0$ due to spin reserval symmetry) the standard linear susceptibility χ_1 remains finite at the spin glass transition, while both χ_3 and $\chi_{\rm SG}$ diverge [1,2]. While $\chi_{\rm SG}$ is convenient for computer simulations, it is not accessible experimentally, and so the entire experimental evidence that the freezing transition of spin glasses is caused by a static phase transition rests on the observed divergence of χ_3 [1,2]. By analogy, for Potts glasses one then also expects that χ_1 remains finite at a possible spin glass transition, while higher order susceptibilites might diverge [6]. Noting that the discrete states of the Potts glass may physically represent discrete orientations of a linear molecule in a diluted (or randomly mixed) molecular crystal [6], χ_2 and χ_3 then get the physical meaning of higher order orientational susceptibilities. Unfortunately, unlike magnetic systems such response functions are not directly accessible in any experiment known to us. Gratifyingly, these response functions can be probed indirectly *via* the rotation-translation coupling, applying a shear field that orients the molecule in a preferred direction indeed a divergent nonlinear response function seems to have been observed [24].

Finally, the dynamic quantity that will be studied is the time-dependent Edwards-Anderson order parameter $q(t)$, which is nothing else but the time-displaced autocorrelation function of the Potts spins,

$$q(t) = \frac{1}{N}\sum_i \left[\langle \mathbf{S}_i(0)\cdot\mathbf{S}_i(t)\rangle_T\right]_{\rm av}. \tag{13}$$

Note that as usual in Monte Carlo sampling dynamics is associated to the model in terms of the master equation that describes the Markov process involved [1,25]. In the present work the "heat bath" algorithm is used, and the unit of time is one attempted Monte Carlo step per Potts spin (MCS), while units of temperature are $3/2\ J/k_{\rm B}$ {remember $J = 2/3\ \hat{J}$, *cf.* Eqs. (1, 4)}. In the following we take $k_{\rm B} \equiv 1$.

Before turning to a description of our results, we recall the equilibration criteria that have been used, following Bhatt *et al.* [7–9,16]. For this purpose, one carries out Monte Carlo runs always for two identical replicas 1, 2 of the model with an identical bond configuration, considering the overlap $\tilde{q}^{\mu\nu}(t)$ of their spin configuration:

$$\tilde{q}^{\mu\nu}(t) = \frac{1}{N}\sum_{i=1}^{N} S_{i,1}^{\mu}(t)S_{i,2}^{\nu}(t). \tag{14}$$

We form a mean square spin glass order parameter from equation (14) defining

$$\tilde{q}^2(t) = \left[\sum_{\mu,\nu}\{\tilde{q}^{\mu\nu}(t)\}^2\right]_{\rm av}, \tag{15}$$

and compare this quantity with the overlap of the spin configuration at time t in one replica with the spin configuration in the same replica at time $2t$,

$$\hat{q}^2(t) = \left[\sum_{\mu,\nu}\{\hat{q}^{\mu\nu}(t)\}^2\right]_{\rm av}, \tag{16}$$

where

$$\hat{q}^{\mu\nu}(t) = \frac{1}{N}\sum_{i=1}^{N} S_{i,1}^{\mu}(t)S_{i,1}^{\nu}(2t). \tag{17}$$

Choosing at $t = 0$ an initial spin configuration at random, it is clear that $\tilde{q}^2(0) = 0$, while $\hat{q}^2 = 1$. On the other hand, both expressions converge to the same quantity in thermal equilibrium, namely,

$$\tilde{q}^2(t\to\infty) = \hat{q}^2(t\to\infty) = \frac{\chi_{\rm SG}}{N}\cdot \tag{18}$$

Thus, anticipating that the relaxation of these quantities towards equilibrium is monotonic in time, $\tilde{q}^2(t)$ approaches the limit in equation (18) from below, while $\hat{q}^2(t)$ approaches it from above. This expectation is indeed consistent with observation, and for the temperatures studied ($T \geq 0.6$ in the units specified above) $t = 300\ 000$ MCS turned out safely sufficient for equilibration. As a consequence, runs of a length 4.3 million MCS were carried out, and the first 300 000 MCS omitted from the averaging.

3 Static properties

We start with a discussion of the correlation function and correlation length $\xi_{\rm SG}(T)$, since for all what follows it is crucial that our choice $L = 16$ (in comparison with simulations of "pure" systems without quenched disorder this is still rather small! [26]) does in fact satisfy $\xi_{\rm SG}(T) \ll L$. Figure 1 shows a semilog plot of the spin glass correlation function $g(r)$ *versus* distance r — straight lines on this plot hence are indicative of an exponential decay, $g(r) \propto \exp(-r/\xi_{\rm SG}(T))$. It is seen that at all temperatures studied $g(r)$ has decayed to very small values after a few lattice spacings. Clearly, such small correlations are hard to estimate with meaningful accuracy (to improve the accuracy in particular a larger sample of random bond configurations would be necessary).

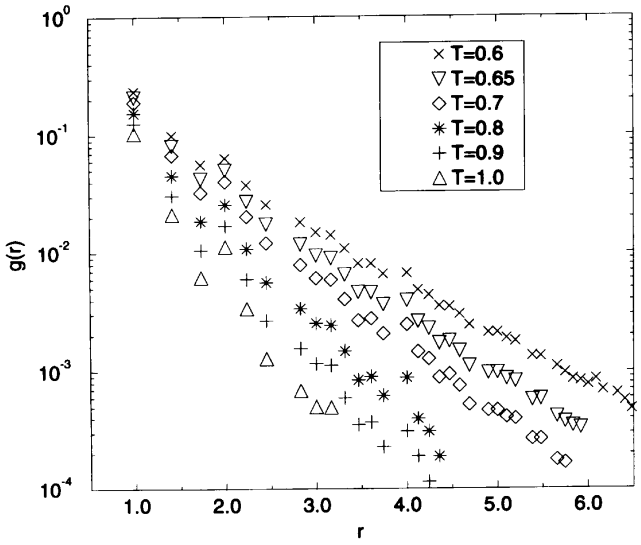

Fig. 1. Plot of the spin glass correlation function $g(r)$ (Eq. (5)) as a function of distance r. Six different temperatures are distinguished by different symbols.

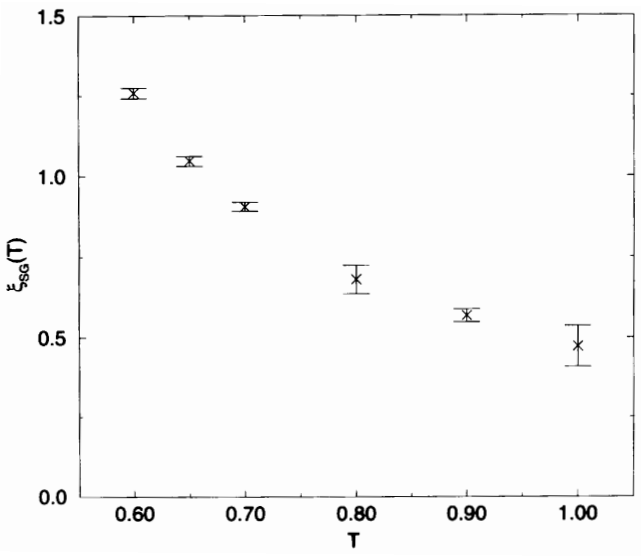

Fig. 2. Log-log plot of the spin glass correlation length $\xi_{\rm SG}(T)$ *versus* temperature.

This "noise" of $g(r)$ for such intermediate values of r make an application of equation (6) difficult, since the summation over distances requires an upper cutoff, and the integration weight $\mathrm{d}^3r\, r^2$ magnifies the noise near the cutoff, a straightforward use of equation (6) thus leads to somewhat imprecise results. We found that a reasonable compromise is to fit an exponential function to the data in Figure 1 for $r \geq 3$ and $T \leq 0.8$ and use this fitted function to estimate the contribution of $r \geq 3$ in equation (6), while for $r < 3$ the data are explicitly used in equation (6). In this way rather stable results for $\xi_{\rm SG}(T)$ are obtained, which are shown in Figure 2 (these data differ only slightly from $\xi_{\rm SG}(T)$ defined from a simple fit of an exponential function to all the data on $g(r)$ [27]). While

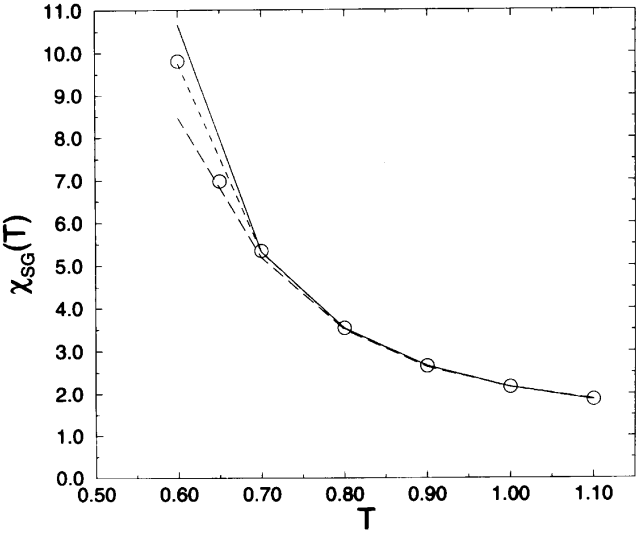

Fig. 3. Plot of $\chi_{\rm SG}(T)$ *vs.* T. Circles are present data (using $L = 16$), while broken curves show data of Scheucher and Reger [8]: $L = 6$ (lower broken curve) and $L = 10$ (upper broken curve). Full curve is the extrapolation to $L = \infty$, obtained in reference [8] from finite size scaling methods. Note that in reference [8] no calculations were carried out at $T = 0.65$, and thus we have connected the results of reference [8] for $T = 0.7$ and $T = 0.6$ by straight lines for simplicity: thus the small discrepancy at $T = 0.65$ presumably is not relevant.

for isotropic orientational glass models related data for $\xi_{\rm SG}(T)$ were compatible with a straight line on a log-log plot of $\xi_{\rm SG}(T)$ *vs.* T [28], this is not the case here, at least over the temperature range shown. Now the scenarios that one wishes to distinguish are [6–9,20]

$$\xi_{\rm SG}(T) \propto \begin{cases} |T - T_{\rm g}|^{-\nu}, & \text{for } d > d_{\rm l}, \\ \exp(C/T^{\sigma}), & \text{for } d = d_{\rm l}, \\ T^{-\nu_0}, & \text{for } d < d_{\rm l}. \end{cases} \tag{19}$$

Unfortunately, the values of $\xi_{\rm SG}(T)$ in the temperature range shown are rather small, and increase by a factor of about 2.5 only: thus it is possible to fit these data to the first two alternatives about equally well: but then $T_{\rm g} \leq 0.3$, *i.e.* a factor of two lower than the lowest temperature used, therefore, this cannot be taken as an evidence for a nonzero glass transition temperature $T_{\rm g}$. Even the third alternative, $\xi_{\rm SG}(T) \propto T^{-\nu_0}$, is not ruled out, despite of the curvature in Figure 2, since it is possible that the asymptotic regime where such a power law holds is only reached for $T \leq 0.6$. In view of these ambiguities, no statement about the exponents ν or σ or ν_0 in equation (19) is possible, of course.

Fortunately, the data for the spin glass susceptibility $\chi_{\rm SG}(T)$ are better behaved (Fig. 3) and in excellent agreement with previous work [8] on smaller lattices. As expected, the data are compatible with the exponential divergence [20]

$$\chi_{\rm SG}(T) \propto \exp(c/T^{\sigma}) \tag{20}$$

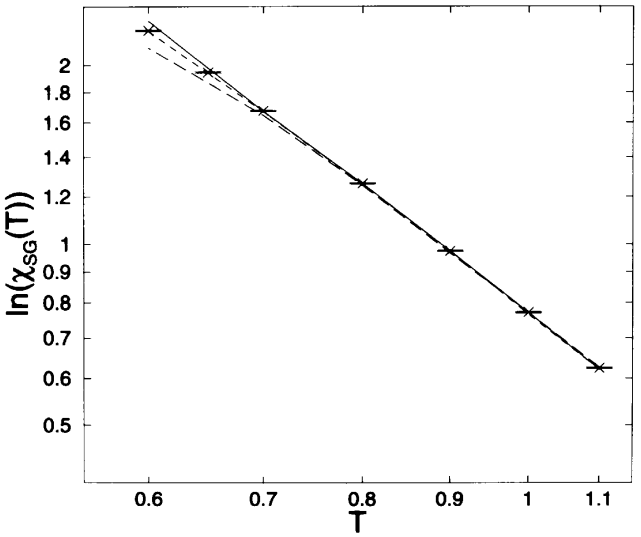

Fig. 4. Log-log plot of $\ln(\chi_{\rm SG}(T))$ *versus* T, to provide evidence for equation (20), which is a straight line at this plot. The present data are indicated by crosses with horizontal error bars (errors are smaller than the size of the crosses!). Broken curves indicate data of reference [8] for $L = 6$ (lower curve) and $L = 10$ (upper curve), respectively, while full straight line is the extrapolation obtained in reference [8] from finite size scaling methods.

where c is a constant and the exponent $\sigma = 2$ (Fig. 4).

While the data presented so far are compatible with reference [8] and thus confirm that the analysis presented by Scheucher and Reger [8] is correct, we present in Figure 5 the quantities χ_1, χ_2 and χ_3 (Eqs. (10-12)) that have not been considered in this reference. Studying the magnetic equation of state, Haas *et al.* [17] were the first to consider these quantities but they obtained qualitatively similar results for χ_1 only: for χ_2 they predicted a decrease with decreasing temperature, with a change of sign at a nonzero temperature, unlike the monotonic increase found here. Clearly, the origin of this qualitative discrepancy requires further study. While there is no problem obtaining χ_1 from fluctuation relations, the huge error bars for χ_2 and χ_3 in Figures 5b, c indicate that the straightforward use of equations (11, 12) is not a very useful method either, and one has to seek for improved estimators with a reduced variance to make further progress. While a quantitative comparison with the results of Haas *et al.* [17] is not possible, since the latter authors considered a Gaussian bond distribution rather than the $\pm J$ distribution, a qualitatively different temperature dependence of χ_2 and χ_3 clearly is very unexpected.

4 Dynamic properties

Apart from early work on the dynamics of the Potts glass with Gaussian bond distribution [15], analysis of the decay of $q(t)$ for Potts glasses has found no attention. We present here data for $q(t)$ in Figure 6 which are of similar statistical quality as the data of Ogielski [14] for the $\pm J$

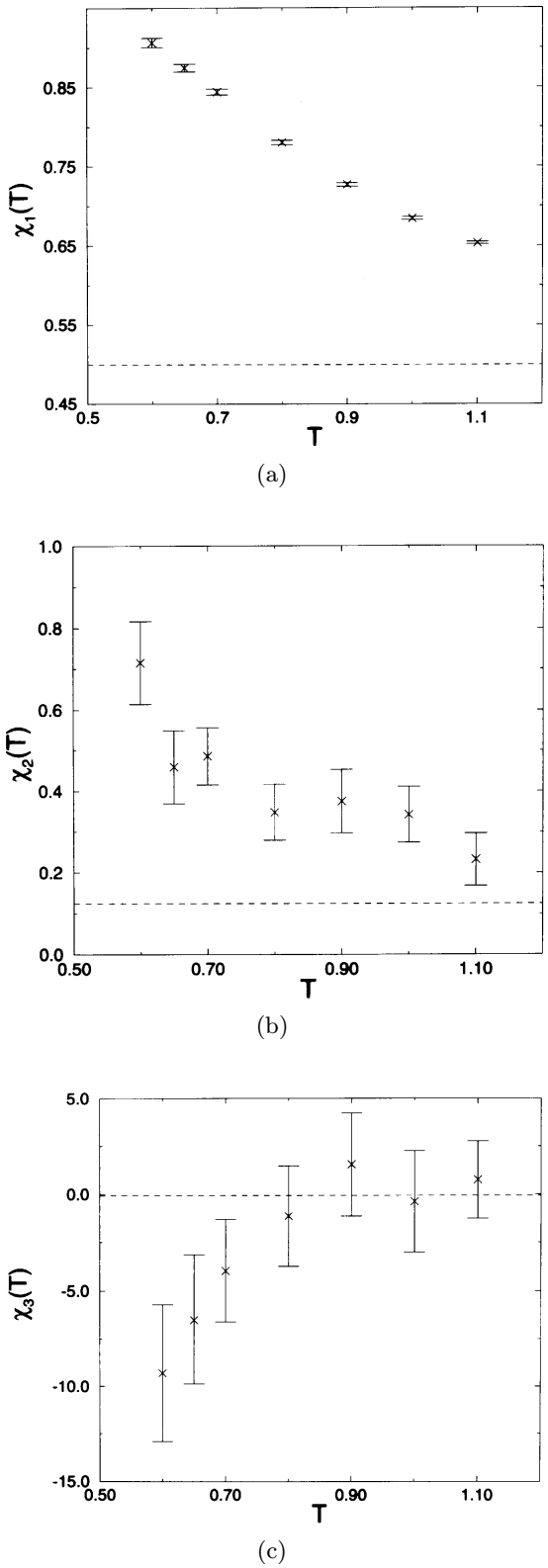

Fig. 5. Ferromagnetic susceptibilities χ_1 (a), χ_2 (b) and χ_3 (c) plotted *vs.* temperature. Horizontal broken lines show limiting values of these susceptibilites for $T \to \infty$, as derived by Haas *et al.* [17] (note the different normalization of the field chosen here).

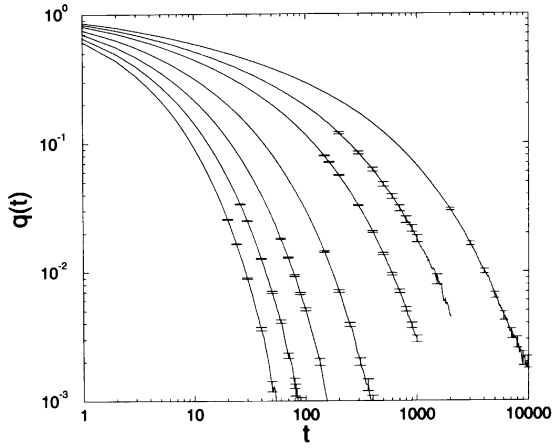

(a)

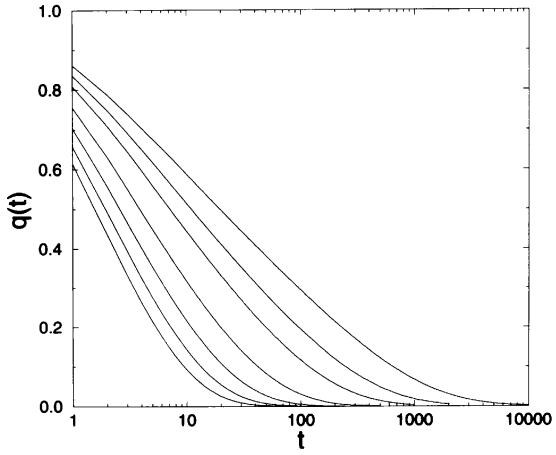

(b)

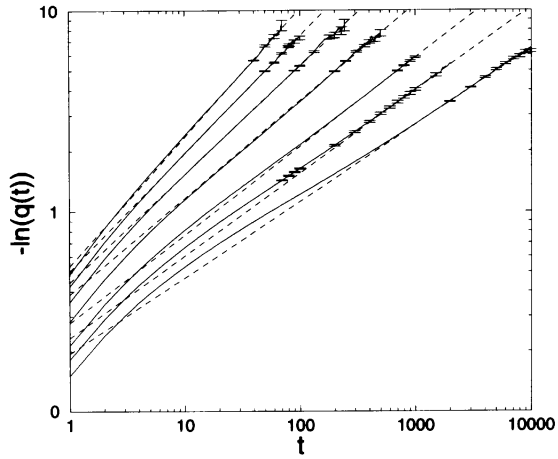

(c)

Fig. 6. (a) Log-log plot of $q(t)$ *vs.* t (in units of MCS), for the temperatures (from left to right) $T = 1.1$, 1.0, 0.9, 0.8, 0.7, 0.65 and 0.60. At late times some examples of error bars are indicated. (b) Linear plot of $q(t)$ *vs.* the logarithm of time, for the same temperatures as in part (a). (c) Log-log plot of $-\ln(q(t))$ *vs.* t, for the same temperatures as in (a). Broken straight lines indicate fits to the Kohlrausch stretched exponential function, equation (21).

Ising spin glass. Figure 6a clearly shows that a power law decay is never a good description of the data over an extended regime of time, unlike the Ising spin glass, where a power law takes over for T near $T_{\rm g}$, the temperature of the spin glass transition. This different behavior may again reflect the fact that $T_{\rm g} = 0$ for the Potts glass, unlike the Ising spin glass, however. A linear plot of $q(t)$ *vs.* time on a logarithmic scale (Fig. 6b) shows that over an intermediate time scale the data perhaps are compatible with a logarithmic decay — but the extent of this regime is not large enough to be really suggestive. Finally, Figure 6c tests the ubiquitous Kohlrausch law,

$$q(t) \propto \exp\{-(t/\tau)^y\}. \tag{21}$$

While equation (21) certainly can describe the data over one or two decades in time, at early times there are clear deviations, and certainly equation (21) is not exact but only a convenient interpolation formula.

If one takes equation (21) seriously, it is of interest to consider the temperature dependence of the parameters τ and y (Fig. 7). Similar to previous results for the Gaussian Potts glass [15] and isotropic quadrupolar glasses [28], one observes a dramatic increase of τ and a distinct decrease of y as the temperature is lowered. In fact, it is conceivable (though the data certainly do not "prove" it) that $y(T) \propto T$ at low temperatures.

As always in glassy systems [1–6], the analysis of the precise temperature dependence of the relaxation time is difficult (Fig. 8). In order to not only rely on the Kohlrausch fit, we have also considered a relaxation time defined from the integral of $q(t)$,

$$\tau_{\rm av} = \int_0^\infty q(t){\rm d}t. \tag{22}$$

Figure 8a compares the temperature dependence of τ and $\tau_{\rm av}$ on a log-log plot. It is seen that the general trend is similar, and since the uncertainties of the fit to equation (21) may affect the accuracy of τ, we concentrate on $\tau_{\rm av}$ in the following. The rather pronounced curvature on the log-log plot in Figure 8a makes a power law divergence of τ and $\tau_{\rm av}$ at zero temperature clearly rather unlikely. However, allowing a nonzero $T_{\rm g}$ it is possible to obtain "good" straight lines on the log-log plot (Fig. 8b). But it is evident that there is no clear preference for one particular value of $T_{\rm g}$; although linearity is best for $T_{\rm g} = 0.45$ the range of the temperature distance, $0.23 \leq 1 - T_{\rm g}/T \leq 0.6$, is so remote from $T_{\rm g}$, that this "agreement" with a power law cannot be taken as a proof of the latter. This point is re-iterated by Figure 8c, where the prediction of McMillan [20], for the dynamic of spin glass systems at the lower critical dimension,

$$\ln \tau \propto T^{-(\sigma+1)} = T^{-3},\ T \to 0, \tag{23}$$

is tested. It is found that the data are nicely compatible with a relation $\ln \tau \propto T^{-z}$ (or $\ln \tau_{\rm av} \propto T^{-z'}$ respectively), but the exponents z, z' do not have the theoretical value $z = z' = \sigma + 1 = 3$ but are slightly smaller. Of course,

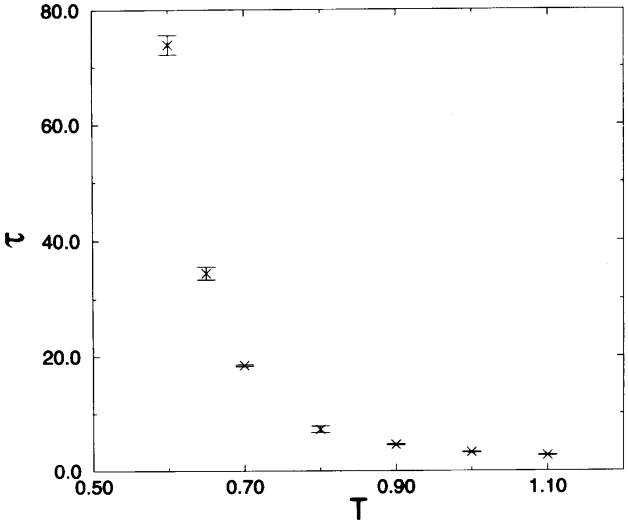

(a)

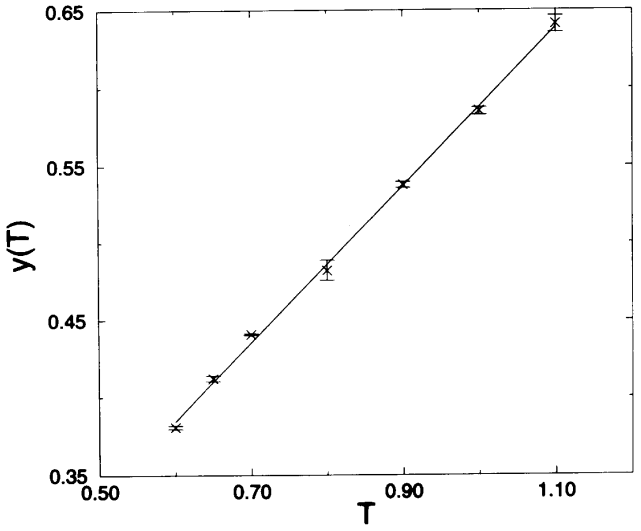

(b)

Fig. 7. (a) Plot of the relaxation time τ, as extracted from the fit of the data to equation (21) in Figure 6c, as function of temperature. (b) Plot of the exponent y, as extracted from the fit of the data in Figure 6c to equation (21), as function of temperature. Straight line indicates that $y(T)$ is compatible with a linear temperature dependence.

we can by no means rule out that equation (23) will be observed if data at lower temperatures actually would become available. However, it is slightly disturbing that in a temperature regime where the result for the static spin glass susceptiblity $\{\ln \chi_{\rm SG} \propto T^{-\sigma} = T^{-2}$ [20]$\}$ already is verified the relaxation time does not yet agree with the theoretical prediction, equation (23).

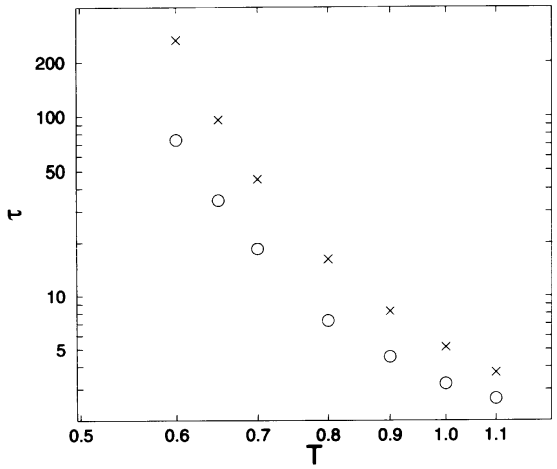

(a)

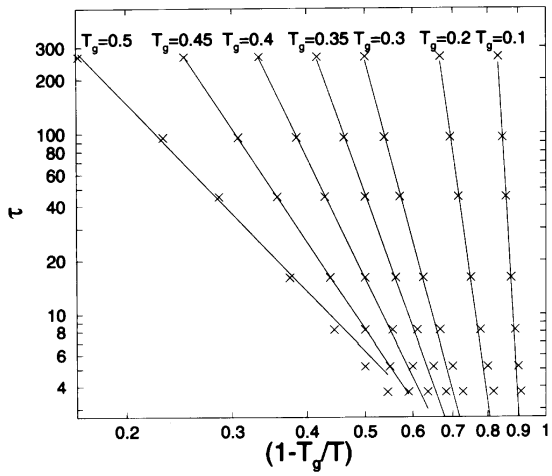

(b)

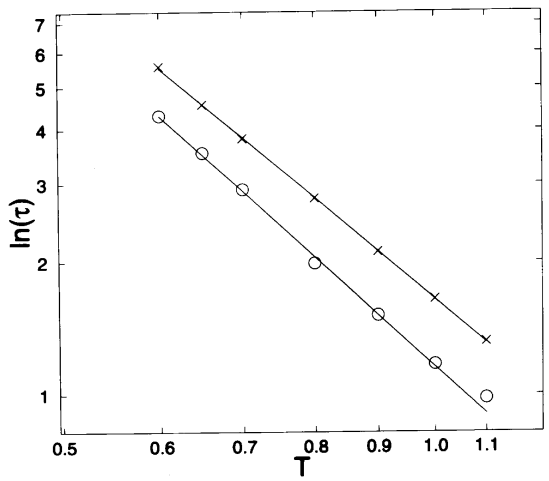

(c)

Fig. 8. (a) Log-log plot τ (circles) and $\tau_{\rm av}$ (crosses) *vs.* temperature. (b) Log-log plot of $\tau_{\rm a}$ *vs.* $1-T_{\rm g}/T$, for 7 trial choices of $T_{\rm g}$ as indicated. (c) Log-log plot of $\ln \tau$ (circles) and $\ln \tau_{\rm av}$ (crosses) *vs.* temperature. Straight lines indicate relations $\ln \tau \propto T^{-z}$, $\ln \tau_{\rm av} \propto T^{-z'}$, with exponents $z = 2.6$, $z' = 2.37$.

5 Discussion

The present work has filled a gap in the research on Potts spin glasses, by presenting a largescale Monte Carlo study of well-equilibrated samples in the high temperature regime for the $\pm J$ three-dimensional three-state Potts glass. Our static results for the spin glass correlation length and spin glass susceptibility confirm a previous finite size scaling study of Scheucher and Reger [8], that has suggested a zero temperature transition with an exponential divergence, $\chi_{\rm SG} \propto \exp(cT^{-\sigma})$ with $\sigma = 2$, although a glass transition at a low but non-zero temperature (described by conventional power laws) still cannot be ruled out.

We also discuss the susceptibilities χ_1, χ_2, χ_3 describing the response to a uniform field, but huge fluctuations prevent us from making any statements on the nature of possible divergences of these response functions as $T \to 0$. More efficient sampling techniques for these quantities are highly desirable but not yet available.

The behavior of the time-dependent Edwards-Anderson order parameter $q(t)$ is qualitatively similar to the Ising spin glass [14] and isotropic quadrupolar glasses [28] but there are differences in quantitative detail. We find that $q(t)$ is compatible with a Kohlrausch stretched exponential, but do not find a power law prefactor. The Kohlrausch exponent seems to decrease strongly with decreasing temperature. The relaxation times are clearly incompatible with a simple power law divergence at zero temperature, unlike the isotropic quadrupolar glasses [28], but a power law divergence at a nonzero $T_{\rm g}$ cannot be ruled out, and is a similar good fit to the data as the McMillan [20] prediction $\ln \tau \propto T^{-z}$, if in the latter relation z is adjusted as an effective exponent (about 20% smaller than the theoretically expected value $z = \sigma + 1 = 3$).

Thus the present work has completed the current picture of Potts glasses somewhat, but open questions clearly remain!

M.R. thanks Prof. H. Monien (Univ. Bonn) for support and stimulating conversations. P.N. is supported by the DFG through a Heisenberg fellowship. This research was carried out in the framework of Sonderforschungsbereich 262 of the DFG.

References

1. K. Binder, A.P. Young, Rev. Mod. Phys. **58,** 801 (1986)
2. K.H. Fischer, J.Y. Hertz, *Spin Glasses* (Cambridge Univ. Press, Cambridge, 1991)
3. M. Mezard, G. Parisi, M Virasoro, *Spin Glass Theory and Beyond* (World Scientific, Singapore, 1987)
4. A.P. Young, *Spin Glasses and Random Fields* (World Scientific, Singapore, 1997)
5. For reviews, see K. Binder, in reference [4], and reference [6].
6. K. Binder, J.D. Reger, Adv. Phys. **41,** 547 (1992).
7. M. Scheucher, J.D. Reger, K. Binder, A.P. Young, Phys. Rev. B **42,** 6881 (1990).
8. M. Scheucher, J.D. Reger, Phys. Rev. B **45,** 2499 (1992).
9. M. Scheucher, J.D. Reger, Z. Phys. B **91,** 383 (1993).
10. O. Dillmann, W. Janke, K. Binder, preprint
11. D.J. Gross, I. Kanter, H. Sompolinsky, Phys. Rev. Lett. **55,** 304 (1985).
12. For recent reviews on finite size scaling in general, see V. Privman, *Finite Size Scaling and the Numerical Simulation of Statistical Systems* (World Scientific, Singapore 1990), and K. Binder, in *Computational Methods in Field Theory*, edited by H. Gausterer, C.B. Lang (Springer, Berlin, 1992), p. 59.
13. A.T. Ogielski, I. Morgenstern, Phys. Rev. Lett. **54,** 928 (1985).
14. A.T. Ogielski, Phys. Rev. B **32,** 7384 (1985).
15. H.-O. Carmesin, K. Binder, J. Phys. A: Math. Gen. **21,** 4053 (1988).
16. R.N. Bhatt, A.P. Young, Phys. Rev. B **37,** 3606 (1988).
17. F.F. Haas, K. Vollmayr, K. Binder, Z. Phys. B **99,** 393 (1996).
18. S.F. Edwards, P.W. Anderson, J. Phys. F **5,** 965 (1975).
19. K. Binder, Z. Phys. B **26,** 339 (1977).
20. W.L. McMillan, J. Phys. C: Solid State Phys. **17,** 3179 (1984).
21. R.B. Potts, Proc. Camb. Philos. Soc. **48,** 106 (1952).
22. For a review of the Potts model, see F.Y. Wu, Rev. Mod. Phys. **54,** 235 (1982).
23. R.K.P. Zia, D.J. Wallace, J. Phys. A: Math. Gen. **8,** 1495 (1975).
24. J. Hessinger, K. Knorr, Ferroelectrics **29,** 127 (1992).
25. K. Binder, D.W. Heermann, *Monte-Carlo Simulation in Statistical Physics: An Introduction* (Springer, Berlin, 1988, 1992)
26. B. Dünweg, in *Monte-Carlo and Molecular Dynamics of Condensed Matter Systems*, edited by K. Binder, G. Ciccotti, (Societa Italiana di Fisica, Bologna 1996), p. 215.
27. M. Reuhl, Diplomarbeit (Bonn 1997, unpublished)
28. D. Hammes, H.-O. Carmesin, K. Binder, Z. Phys. B **76,** 115 (1989).